

## ORIGINAL RESEARCH

## Columnar-Lined Esophagus Develops via Wound Repair in a Surgical Model of Reflux Esophagitis



Agoston T. Agoston,<sup>1,\*</sup> Thai H. Pham,<sup>2,\*</sup> Robert D. Odze,<sup>1</sup> David H. Wang,<sup>3,4</sup> Kiron M. Das,<sup>5</sup> Stuart J. Spechler,<sup>6</sup> and Rhonda F. Souza<sup>6</sup>

<sup>1</sup>Department of Pathology, Brigham and Women's Hospital, Harvard Medical School, Boston, Massachusetts; <sup>2</sup>Department of Surgery, <sup>3</sup>Department of Medicine, VA North Texas Health Care System, <sup>4</sup>Harold C. Simmons Comprehensive Cancer Center, University of Texas Southwestern Medical Center, Dallas, Texas; <sup>5</sup>Division of Gastroenterology, Department of Medicine, Rutgers Robert Wood Johnson Medical School, New Brunswick, New Jersey; <sup>6</sup>Department of Medicine, Center for Esophageal Diseases, Baylor University Medical Center, Center for Esophageal Research, Baylor Scott and White Research Institute, Dallas, Texas

## SUMMARY

After esophagojejunostomy, rodents develop ulcerative esophagitis and a columnar esophageal lining widely assumed to develop from progenitor cell reprogramming. This analysis study of early events in this process shows that this metaplastic, columnar-lined esophagus develops via wound healing rather than epithelial reprogramming.

**BACKGROUND & AIMS:** After esophagojejunostomy, rodents develop reflux esophagitis and a columnar-lined esophagus with features of Barrett's metaplasia. This rodent columnar-lined esophagus has been proposed to develop from cellular reprogramming of progenitor cells, but studies on early columnar-lined esophagus development are lacking. We performed a systematic, histologic, and immunophenotypic analysis of columnar-lined esophagus development in rats after esophagojejunostomy.

**METHODS:** At various times after esophagojejunostomy in 52 rats, the esophagus was removed and tissue sections were evaluated for type, location, and length of columnar lining. Molecular characteristics were evaluated by immunohistochemistry and immunofluorescence.

**RESULTS:** At week 2, ulceration was seen in esophageal squamous epithelium, starting distally at the esophagojejunostomy anastomosis. Re-epithelialization of the distal ulcer segment occurred via proliferation and expansion of immature-appearing glands budding directly off jejunal crypts, characteristic of wound healing. The columnar-lined esophagus's immunoprofile was similar to jejunal crypt epithelium, and columnar-lined esophagus length increased significantly from 0.15 mm ( $\pm 0.1$  SEM) at 2 weeks to 5.22 mm ( $\pm 0.37$ ) at 32 weeks. Neoglands were found within esophageal ulcer beds, and spindle-shaped cells expressing epithelial-mesenchymal transition markers were found at the columnar-lined esophagus's leading edge. Only proliferative squamous epithelium was found at the proximal ulcer border.

**CONCLUSIONS:** After esophagojejunostomy in rats, metaplastic columnar-lined esophagus develops via a wound healing process that does not appear to involve cellular reprogramming of progenitor cells. This process involves EMT-associated

migration of jejunal cells into the esophagus, where they likely have a competitive advantage over squamous cells in the setting of ongoing gastroesophageal reflux disease. (*Cell Mol Gastroenterol Hepatol* 2018;6:389–404; <https://doi.org/10.1016/j.jcmgh.2018.06.007>)

**Keywords:** Gastroesophageal Reflux; Barrett's Esophagus; Epithelial-Mesenchymal Transition.

See editorial on page 468.

Barrett's esophagus, the condition in which an abnormal columnar mucosa with both gastric and intestinal features replaces esophageal squamous mucosa damaged by gastroesophageal reflux disease (GERD),<sup>1,2</sup> is a major risk factor for esophageal adenocarcinoma.<sup>3,4</sup> The pathogenesis of Barrett's esophagus is judged to involve GERD-induced alterations of key developmental transcription factors expressed by the cells that give rise to metaplastic columnar mucosa. The identity of those Barrett's progenitor cells is not known, but a number of potential candidates recently were reported (reviewed by Wang and Souza<sup>5</sup>). It has been proposed that GERD might cause mature esophageal squamous cells to transdifferentiate into columnar cells, or cause immature esophageal progenitor cells (in the basal layer of the squamous epithelium or in the ducts of esophageal submucosal glands) to undergo columnar rather than squamous differentiation (a process known as transcommitment) (reviewed

\*Authors share co-first authorship.

**Abbreviations used in this paper:** GERD, gastroesophageal reflux disease; Dcamk1, doublecortin and CaM kinase-like-1; EMT, epithelial-mesenchymal transition; Msi-1, Musashi-1; Muc, mucin; Pdx1, pancreatic and duodenal homeobox 1; Sox, sex determining region Y-box.



Most current article

© 2018 The Authors. Published by Elsevier Inc. on behalf of the AGA Institute. This is an open access article under the CC BY-NC-ND license (<http://creativecommons.org/licenses/by-nc-nd/4.0/>).

2352-345X

<https://doi.org/10.1016/j.jcmgh.2018.06.007>

by Wang and Souza<sup>5</sup>). Some investigators have suggested that Barrett's metaplasia might result from upward migration of stem cells from the gastric cardia,<sup>6</sup> or from proximal expansion of unique populations of residual embryonic cells<sup>7</sup> or transitional basal cells<sup>8</sup> located at the squamocolumnar junction. Other investigators have proposed that circulating bone marrow stem cells that settle in the reflux-damaged esophagus are the Barrett's progenitors.<sup>9</sup>

Animal models, primarily involving rodents, have been used to explore the pathogenesis of Barrett's esophagus. In 1962, Levrat et al<sup>10</sup> reported that they could induce severe ulcerative reflux esophagitis in rats by connecting the duodenum to the esophagus (ie, creating an esophagoduodenostomy). Later, other investigators showed that some rats with reflux esophagitis induced by esophagoduodenostomy or by esophagojejunostomy developed a Barrett's-like columnar lining in the esophagus that was capable of neoplastic progression to dysplasia and adenocarcinoma.<sup>11-13</sup> Although many investigators since then have used esophagojejunostomy in rodents as a model for studying Barrett's metaplasia and its neoplastic progression, none systematically explored the early events whereby reflux esophagitis ultimately results in the development of a columnar-lined esophagus.

In our study, we conducted a systematic investigation of the early histologic events in the development of a columnar-lined esophagus in rats after esophagojejunostomy. These rats developed ulceration in the squamous-lined distal esophagus starting at the anastomotic site and progressing proximally up the esophagus, with subsequent progressive re-epithelialization of the distal portion of the ulcer bed (adjacent to jejunum) by an intestinal type of columnar epithelium. We used immunohistochemical techniques to characterize the native epithelia both proximal and distal to esophageal ulcers (squamous epithelium proximally, jejunal epithelium distally), as well as the cells that appeared to be re-epithelializing the proximal and distal portions of the ulcer bed. We found that the columnar-lined esophagus in this animal model develops via a wound healing process that includes epithelial-mesenchymal transition (EMT) of the intestinal cells at the ulcer edge, and not via genetic reprogramming of progenitor cells. We also found that the squamous epithelium at the proximal ulcer border showed decreased expression of a squamous transcription factor (sex determining region Y-box [Sox]2) while showing increased expression of a columnar transcription factor (Sox9), consistent with the beginning of a metaplastic process, but the cells still maintained their histologic squamous phenotype.

## Results

### *Time Course for the Induction of Esophageal Ulceration and the Development of Columnar Epithelium in the Distal Esophagus*

In the sham-operated control animals, no inflammation, erosion, or ulceration was observed in the distal esophagus at any time point (Figure 1A), and none developed evidence of columnar-lined esophagus at any time point as well. After esophagojejunal anastomosis, ulceration developed in the

distal esophagus starting at the level of the anastomosis distally, and advancing a variable distance proximally (Figure 1B). The squamous epithelium located immediately proximal to the area of ulceration showed increased intraepithelial lymphocytes and neutrophils (without eosinophils). Severe reactive changes were seen in this epithelium, including basal cell hyperplasia, papillary hyperplasia, spongiosis, and surface erosions (Figure 1C). At the distal end of the area of ulceration, at the level of the anastomosis (Figure 1B, left panel), the native jejunal epithelium was intact, but showed expansion, proliferation, and growth of crypt epithelium into the mesenchyme situated underneath the ulcer base. Populations of the crypt epithelium originated from the bases of the native jejunal crypts, which expanded and appeared to grow proximally into the mesenchyme. This neoglandular epithelium was immature in appearance, showing an irregular, angulated, budding architecture and composed of cells with enlarged nuclei, prominent nucleoli, mucin depletion, and increased mitoses. The length of the neoglandular ingrowth increased progressively from 2 to 8, 16, and, ultimately, to 32 weeks after surgery (Figure 2). By 32 weeks after surgery, the neoglandular epithelium advanced to its most proximal extent into the distal esophagus, and showed growth around islands of residual squamous epithelium (Figure 3A and B). The length of neoglandular epithelium, measured from the anastomosis site to its most proximal level (Figure 3A and B), increased progressively from 0.15 mm (SEM,  $\pm 0.1$ ) at 2 weeks to 5.22 mm (SEM,  $\pm 0.37$  mm) at 32 weeks after surgery (Figure 3C). There was a highly significant linear relationship between the length of the neoglandular epithelium in the distal esophagus and the number of weeks after surgery ( $r = 0.94$ ;  $P < .0001$ ) (Figure 3C).

### *Distal Esophageal Neoglandular Epithelium Expresses Markers of Intestinal Differentiation and Pdx1 Similar to Native Jejunal Epithelium*

Immunohistochemical characterization of neoglandular epithelium located immediately proximal to the anastomosis showed features similar to those of the native nonproliferating jejunal epithelium located immediately distal to the anastomosis. The neoglandular epithelium stained positive for all intestinal markers including caudal-related homeobox transcription factor 2 (an intestinal nuclear transcription factor), villin and cluster of differentiation 10 (both markers of small intestinal brush border), and mucin (Muc)2 (an intestinal-specific mucin) (Figure 4A). The neoglandular epithelium also was strongly positive for periodic acid-Schiff/Alcian blue (pH 2.5) staining, indicating the presence of acidic mucin-containing cells (data not shown). Both the neoglandular and native jejunal epithelium were negative for Muc5AC and Muc6 (both gastric epithelial mucin markers), p63 (a squamous epithelial marker), and Das-1 (a marker of human colonic goblet cells) (data not shown).<sup>14</sup> In mouse models of surgically induced reflux esophagitis, expression of Pdx1 (a foregut transcription factor) was used as an index of esophageal columnar metaplasia via cellular reprogramming.<sup>15</sup> In 56% of our rats

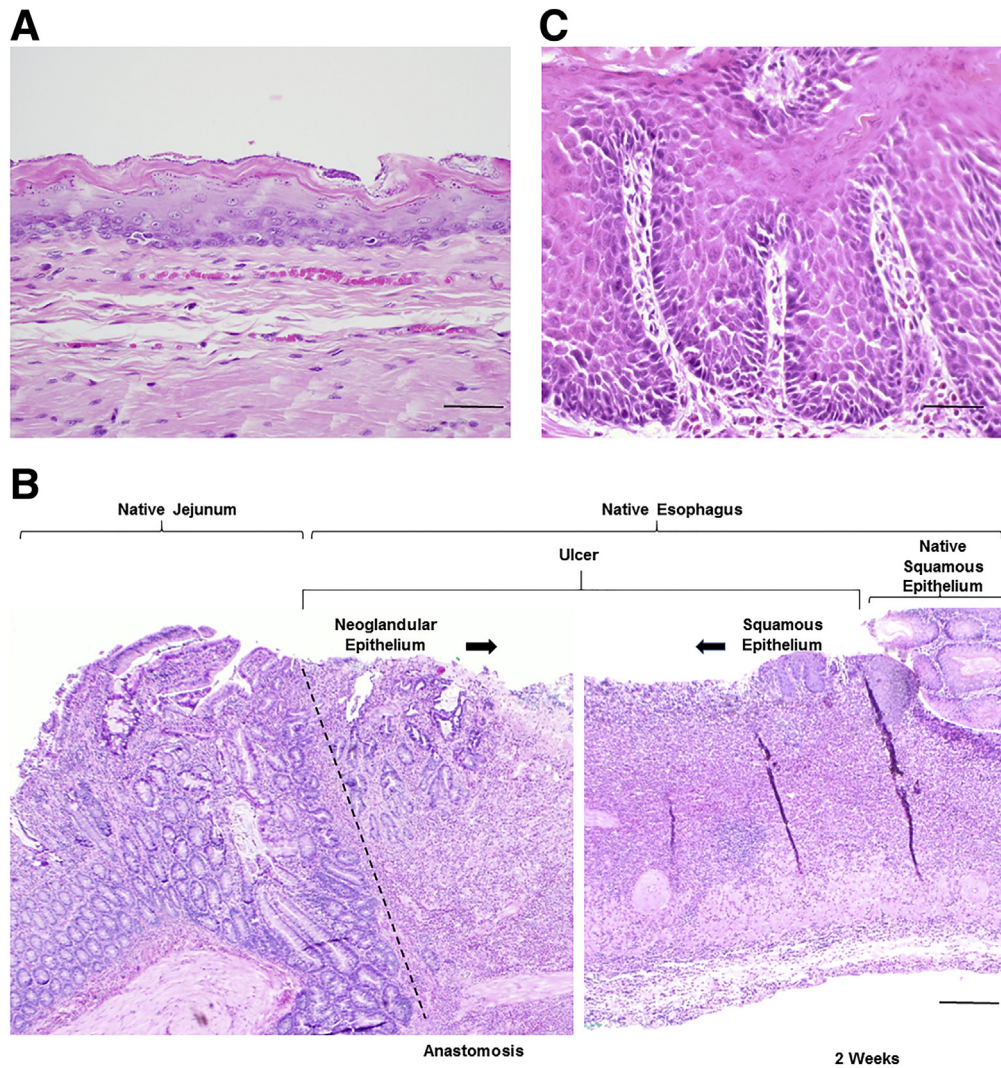


**Figure 1. Distal esophageal ulceration and re-epithelization by a columnar epithelium in animals that underwent an esophagojejunal anastomosis.** (A) Photomicrograph of a sham-operated control animal with no inflammation, erosion, or ulceration observed in the distal esophageal squamous mucosa. *Scale bar: 100  $\mu\text{mol/L}$ .* (B) Photomicrograph of the esophagojejunal anastomosis at 2 weeks after surgery showing ulceration of the distal esophagus, adjacent to the anastomosis. Neoglandular epithelium extends proximally into the distal esophagus from the distal edge of the ulcer, whereas squamous epithelium at the proximal edge of the ulcer shows active esophagitis and regeneration. *Scale bar: 200  $\mu\text{mol/L}$ .* (C) Higher-magnification view of the proximal squamous mucosa showing active esophagitis, lymphocytic, and neutrophilic infiltrates and reactive changes including basal cell hyperplasia, papillary hyperplasia, spongiosis, and erosion. *Scale bar: 40  $\mu\text{mol/L}$ .*

after esophagojejunostomy, both the neoglandular and native jejunal epithelium showed Pdx1 staining of similar intensity (Figure 4B), whereas the remaining 44% showed no staining for Pdx1 in either the neoglandular or native jejunal epithelium. There was no discernable relationship between Pdx1 positivity and any postoperative time point.

#### *Distal Esophageal Neoglandular Epithelium Is Highly Proliferative, Immature, and Expresses Intestinal Stem Cell Markers Musashi-1 and Dcamk1*

In colonic wound healing, wound-associated epithelial cells normally arise from the bases of the crypts and then grow into the ulcerated area of mucosa.<sup>16</sup> We characterized

the epithelium in the deep portions of the native jejunal crypts from where the buds of neoglandular epithelium were derived (the normal proliferative zone where intestinal stem cells reside) using the putative gastrointestinal stem cell markers Musashi-1 (Msi-1) and doublecortin and CaM kinase-like-1 (Dcamk1).<sup>17</sup> Leucine-rich, repeat-containing, G-protein-coupled receptor 5 immunostaining was not performed because prior lineage-tracing studies have shown that Leucine-rich, repeat-containing, G-protein-coupled receptor 5-positive progenitors are not present in the columnar-lined esophagus of mice that had an esophagojejunostomy.<sup>18</sup> As expected, the native deep crypt jejunal epithelium showed positive nuclear staining for Msi-1 at the base of crypts up to approximately the +3 position (the third cell up from the base of the crypt) (Figure 5). Nuclei

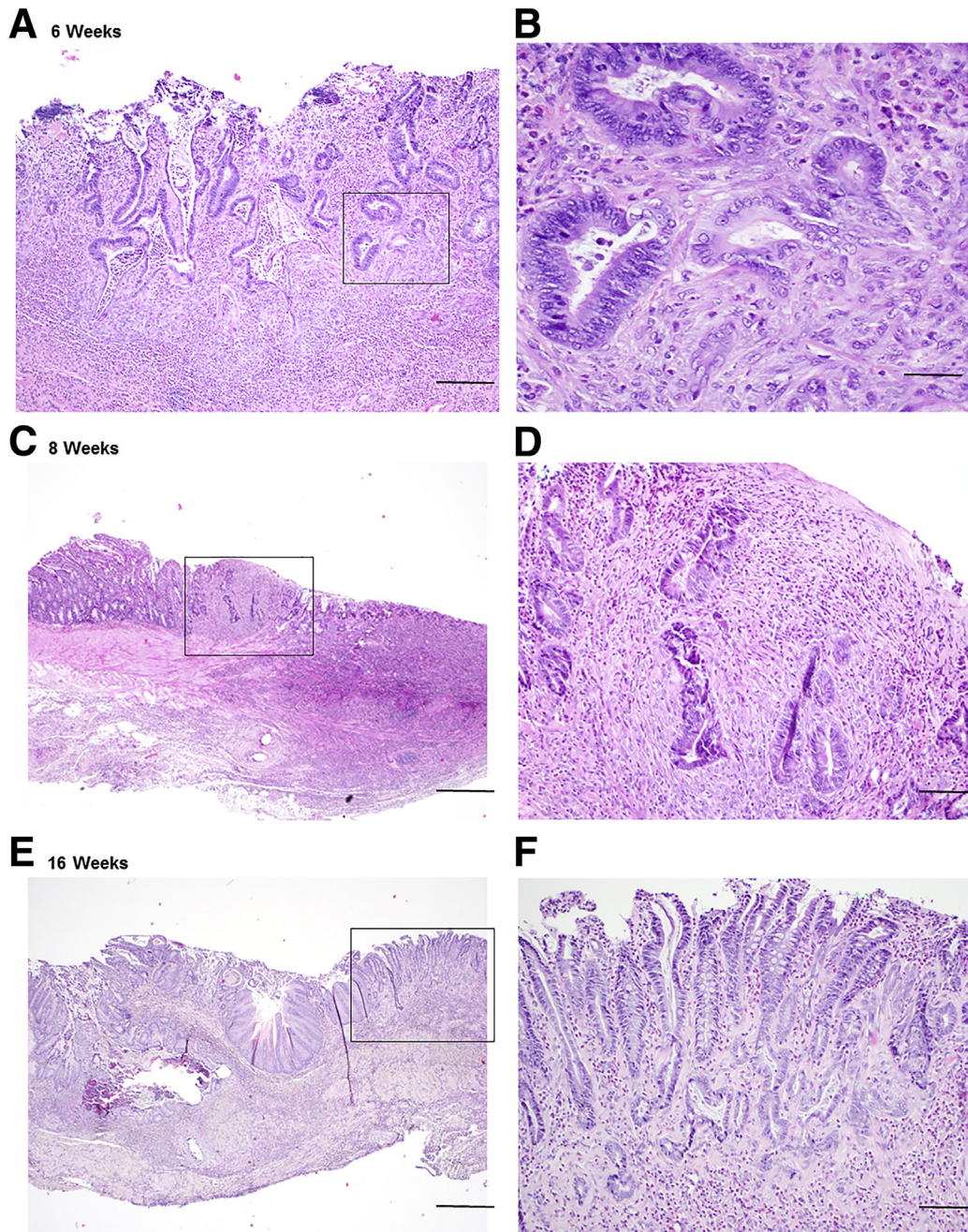


**Figure 2.** Histopathologically, neoglandular epithelium appears immature, showing irregular, angulated, budding proliferating glands comprising cells with increased nuclear-to-cytoplasmic ratios, prominent nucleoli, mucin depletion, and increased mitoses. The glands are present in the mesenchyme deep to the ulcer bed as well. The neoglandular epithelium at 6 weeks, shown at (A) medium power and (B) high power; at 8 weeks, shown at (C) low power and (D) medium power; and at 16 weeks at (E) low power and (F) medium power. Scale bars: (C and E) 200  $\mu\text{mol/L}$ , (A, D, and F) 100  $\mu\text{mol/L}$ , and (B) 40  $\mu\text{mol/L}$ . Note: The boxed areas in A, C, and E are the higher magnification images shown in B, D, and F.

located more superficial to this position in the crypts and the villi were negative for Msi-1 staining. Dcamk11 staining was less well demarcated in the native crypt jejunal epithelium, but predominantly was limited to cells in the crypts (~10%–15%), with rare Dcamk11-positive cells also present in the villi (Figure 5). Unlike native jejunal epithelium in which nuclear staining for Msi-1 was limited to cells at the crypt bases, nuclear staining for Msi-1 was seen

diffusely throughout proliferating neoglandular epithelium (Figure 5). The intensity of Msi-1 staining within the neoglandular epithelium was similar to that observed in the deep crypt bases of the native jejunal epithelium. Similar to native jejunal epithelium, the neoglandular epithelium also showed staining with Dcamk11 (in approximately 15% of cells). As expected, proliferative activity in the normal native jejunal epithelium was limited to the crypt compartment. In

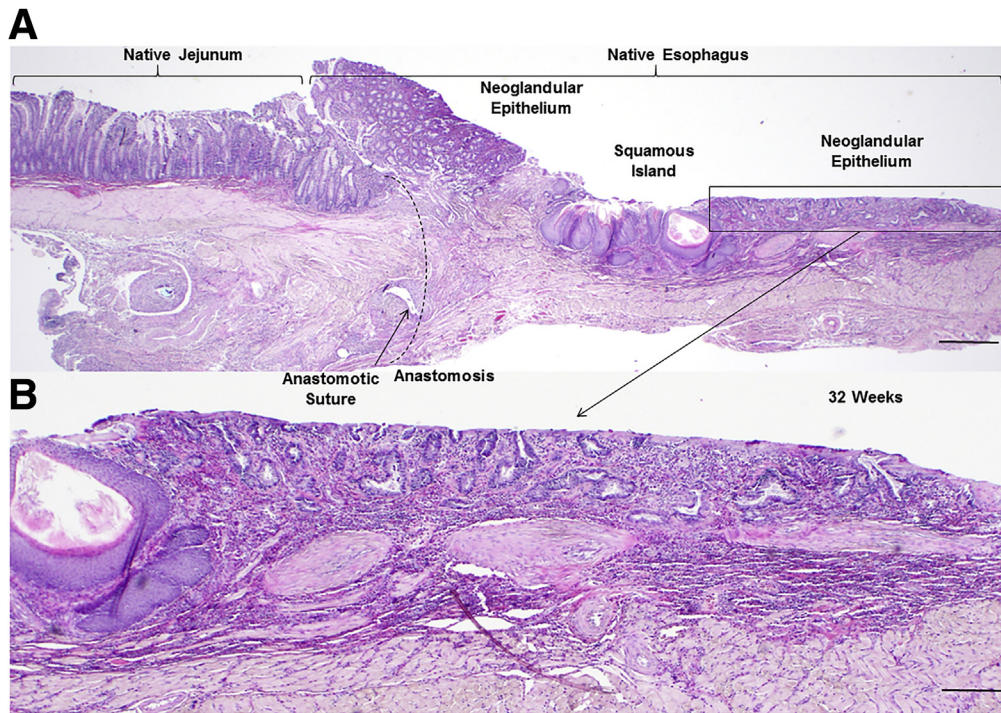


**Figure 3. Growth of neoglandular epithelium into the ulcer bed progressed in a linear fashion.** (A) Photomicrograph of the esophagojejunal anastomosis at 32 weeks postoperatively. Note that the neoglandular epithelium in the distal esophagus has grown around an island of squamous epithelium and has re-epithelialized the majority of the ulcer bed. *Scale bar: 200  $\mu$ mol/L.* (B) Higher-magnification view of the neoglandular epithelium showing irregular, angulated, proliferating glands growing into the base of the ulcer. *Scale bar: 100  $\mu$ mol/L.* (C) Neoglandular epithelium progressed proximally at a growth rate of 0.17 mm/wk. A significant linear relationship ( $r = 0.94$ ) was seen between the length of the neoglandular epithelium and the number of weeks after surgery ( $P < .01$ ).

this region, the Ki-67 proliferative index was approximately 40%–50%. Ki-67 staining was negative in the villi (Figure 5). The proliferating neoglandular epithelium also showed positivity for Ki-67 in approximately 40%–50% of cell nuclei. Overall, these findings suggest that the neoglandular epithelium that extends into the deep mesenchyme of the distal esophageal ulcer is a proliferative immature type of epithelium that is immunohistochemically similar to native jejunal crypt epithelium.

#### *EMT Plays a Role in Re-epithelialization of the Distal Esophageal Ulcer Bed by Proliferating Neoglandular Epithelium*

As discussed earlier, we observed a distinct proliferation and expansion of neoglandular epithelium arising from the bases of crypts in the jejunal epithelium at the level of the anastomosis, and extending into the mesenchyme of the ulcer bed. In some cases, this epithelium appeared to surround islands of residual squamous epithelium. We explored the possibility that this cell migration might have occurred through the process of EMT by immunostaining neoglandular epithelium for E-cadherin (an epithelial cell marker), and for Twist and Snail (both mesenchymal markers found in cells undergoing EMT). We found focal nuclear staining for Twist in a population of spindle-shaped, mesenchymal-like cells located at the proximal leading edge of the neoglandular

epithelium in the ulcer bed (Figure 6, arrows); staining for Snail was negative (data not shown). E-cadherin staining was uniformly positive in neoglandular epithelium in a membranous staining pattern. Interestingly, weak E-cadherin staining also was seen in the spindle-shaped, mesenchymal-like cells in the deep mesenchyme of the ulcer bed (Figure 6, arrows). Double-immunofluorescence staining showed colocalization of nuclear Twist and E-cadherin in the same population of spindle-shaped cells, consistent with an EMT origin (Figure 7).

#### *Esophageal Squamous Epithelium Located at the Ulcer Edge Is Highly Proliferative and Expresses Significantly Higher Levels of Sox9 than Esophageal Squamous Epithelium Located More Proximal to the Ulcer*

We performed immunostaining for Ki-67 and for Sox2 (a marker of basal progenitor cells in the adult esophagus) in the squamous epithelium located at (ie, within 2 mm) the proximal edge of the esophageal ulcer, and also at 5–10 mm proximal to the ulcer edge (Figure 8). In both basal and parabasal cell nuclei of the squamous epithelium located within 2 mm of the ulcer edge, we observed a marked decrease in Sox2 immunostaining compared with basal and parabasal cell nuclei of the more proximal regions of squamous epithelium (Figure 8). The Ki-67 proliferative

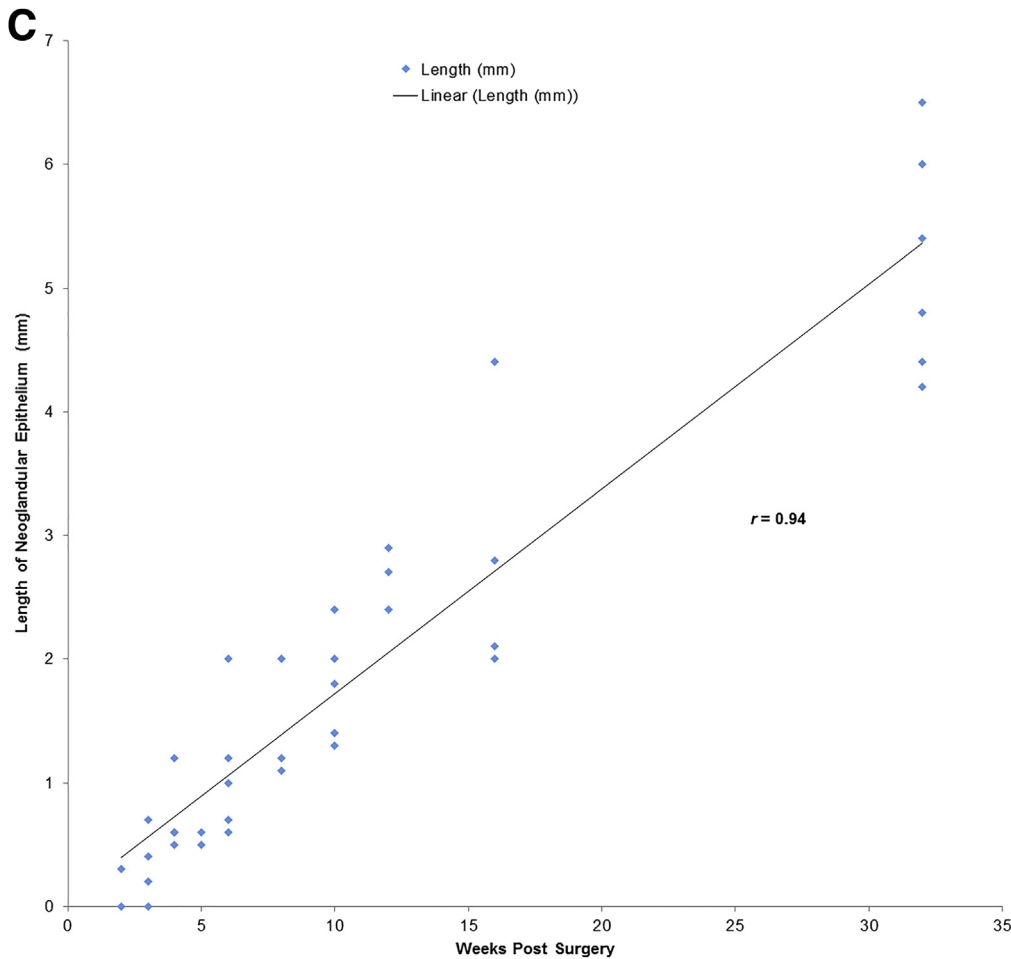


Figure 3. (continued).

index was significantly higher in squamous epithelium at the ulcer edge than in the more proximal squamous epithelium (Figure 8).

Sox9, a marker of progenitor cells in the adult intestine, liver, and pancreas, is expressed in columnar epithelial cells that line the early embryonic esophagus; however, Sox9 expression is switched off in the adult squamous-lined esophagus.<sup>19</sup> We observed a significant increase in Sox9 immunostaining in squamous epithelium located within 2 mm of the ulcer edge compared with the more proximal squamous epithelium (Figure 8). As expected, Sox9 was uniformly positive in both neoglandular epithelium (Figure 8A) and in native jejunal epithelium (data not shown).

## Discussion

Our exploration of the early histologic events in the development of columnar-lined esophagus in rats after esophagojejunostomy has yielded a number of novel findings. Specifically, we have shown that a metaplastic, columnar-lined esophagus appears to develop via a process typical of wound healing in which the distal edge of reflux-induced esophageal ulceration (the edge abutting jejunum)

is populated by an immature neoglandular epithelium that arises directly from crypt bases of the native jejunal epithelium, while the proximal ulcer edge shows expansion and proliferation of squamous epithelium. As would be expected with wound healing from an intestinal source, the leading front of the proliferating neoglandular epithelium shows an immature phenotype and expresses typical intestinal cell markers, and its Pdx1 expression mirrors that of the native jejunum. Furthermore, this advancing front of neoglandular epithelium harbors a population of spindle-shaped, mesenchymal-appearing cells with EMT features including expression of the mesenchymal transcription factor Twist-1 in the same cells that express the epithelial marker E-cadherin only weakly. Finally, we have shown that the length of neoglandular epithelium increases linearly over time. Our findings do not support the hypothesis that intestinal metaplasia in this rodent model develops via cellular reprogramming of progenitor cells. Rather, we have shown that this esophageal intestinal metaplasia arises via a wound healing process in which EMT enables jejunal cells to migrate into the reflux-damaged esophagus, where the intestinal cells likely have a competitive advantage over their squamous counterparts in the setting of ongoing reflux esophagitis.

A

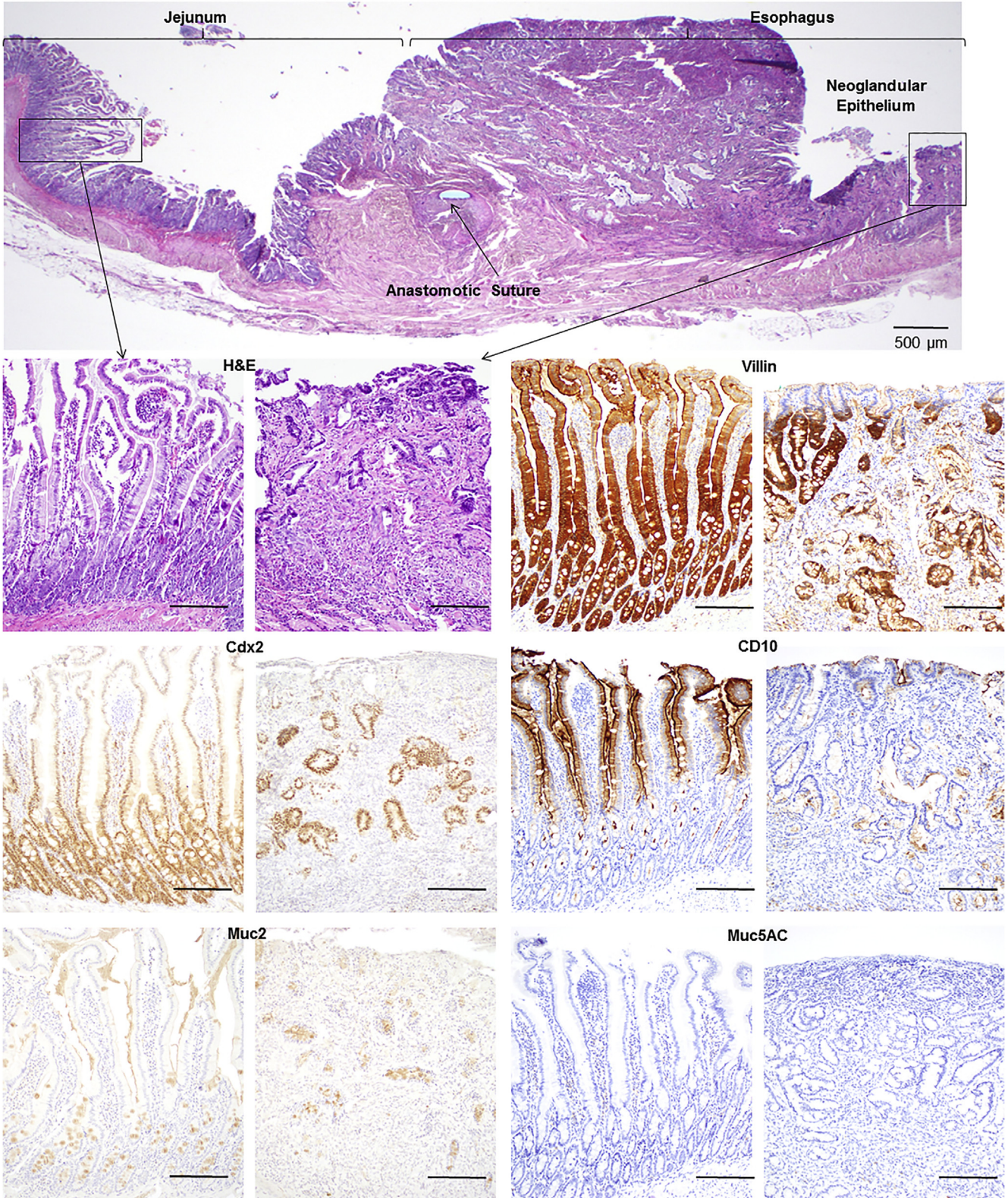


**Figure 4. Neoglandular epithelium in the esophagus expressed markers of intestinal differentiation and Pdx1 similar to that of native jejunal epithelium.** (A) Immunostaining for markers of intestinal and gastric differentiation in native jejunal epithelium (*left side of each pair*) and neoglandular epithelium (*right side of each pair*). Both the jejunal epithelium and neoglandular epithelium stained positively for intestinal markers such as caudal-related homeobox transcription factor (Cdx)2, Muc2, Villin, and cluster of differentiation (CD)10, and negative for gastric markers Muc5AC and Muc6 (not shown). Scale bar: 100  $\mu\text{m}$ . (B) Both the neoglandular epithelium and native jejunal epithelium stained positively for Pdx1. Scale bar: 50  $\mu\text{m}$ .

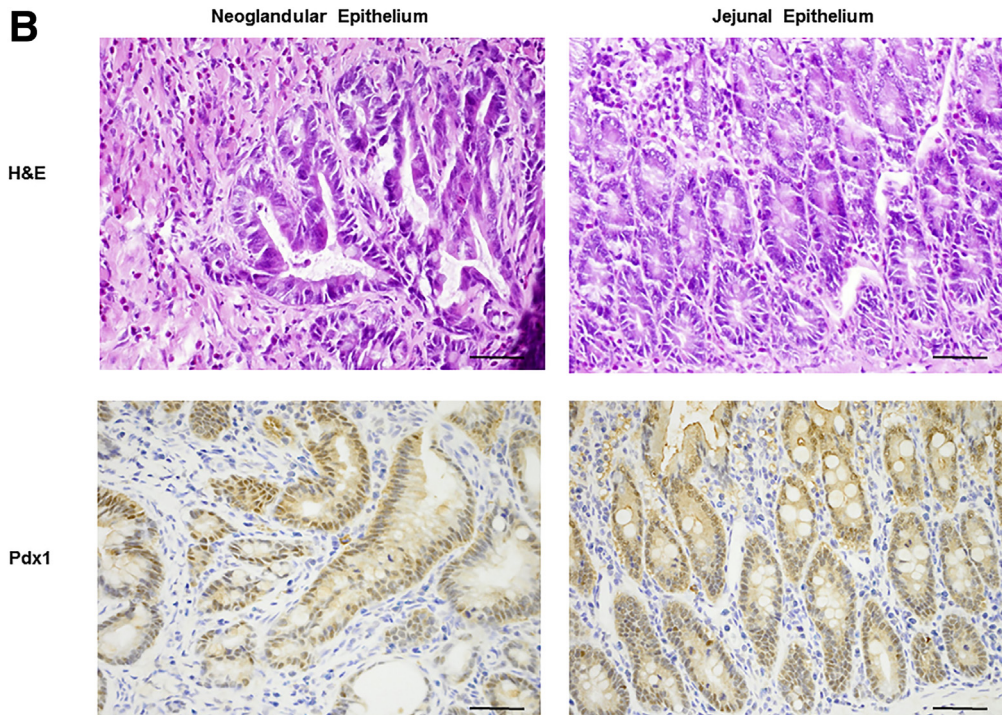


Figure 4. (continued).

As is typical of experimental studies of wound healing in other organs, the few that have focused specifically on esophageal wound healing have involved only a very limited type of mucosal injury that was inflicted by brief exposure to a single noxious agent (eg, acetic acid) on a single type of epithelium (ie, squamous).<sup>20</sup> However, reflux esophagitis often involves extensive esophageal injury inflicted by chronic exposure to a mixture of noxious agents (acid and bile), ultimately leading to a wound that is bordered proximally by squamous epithelium and distally by columnar epithelium. Studies using surgical models to produce reflux esophagitis in rodents generally have focused on the frequency with which columnar epithelium develops or progresses to esophageal adenocarcinoma, or on the similarity of the rodent columnar-lined esophagus to human Barrett's epithelium.<sup>11,21,22</sup> We focused systematically on the healing of esophageal ulcers that were situated between 2 different types of epithelia in the setting of chronic injury.

The area of esophageal ulceration that we observed after esophagojejunostomy in our rats was more extensive than that described in similar mouse and rat models of reflux esophagitis. The reason for this difference is not clear, but we speculate that it is the result of technical aspects of our reflux-inducing surgery. We intentionally fashioned a large anastomotic orifice between the esophagus and jejunum, perhaps larger than that fashioned by other investigators. We suspect that this larger orifice resulted in esophageal exposure to larger volumes of refluxate and, consequently, larger areas of ulceration. Our observation that 62.5% of our animal deaths were caused by pulmonary aspiration supports our contention that these animals experienced high-volume reflux. We found that the rats developed large esophageal ulcers spanning a variable region of the

esophagus, but always starting distally at the level of the anastomosis. If this injury were to be repaired entirely via a squamous-to-columnar metaplastic process, then columnar mucosa would be expected to be found at both the proximal and distal ulcer edges. In contrast, mucosal repair of this large esophageal ulceration by wound healing would be expected to result in proliferative squamous epithelium lining the proximal ulcer wound and proliferative neoglandular epithelium lining the distal ulcer edge, which is precisely what we found.

Squamous cells with an increased Ki-67 proliferative index appeared to grow into the proximal ulcer bed, as would be expected for an epithelium attempting to regenerate via normal wound repair mechanisms.<sup>23</sup> Our observation that ulceration persisted proximal to the neoglandular epithelium at all time points studied suggests that the proliferative squamous cells could not re-epithelialize the ulceration completely in the setting of ongoing reflux caused by esophagojejunostomy. In the distal-most portion of the ulcer bed, we found newly developed neoglandular epithelium proliferating and expanding directly from the native jejunal crypts, and growing proximally into the mesenchyme located underneath the ulcer bed. The immature appearance of the neoglandular epithelium with its irregular, angulated, budding, and proliferating glands is typical of regenerating columnar epithelium found normally at the border of ulcers in the human intestinal tract. The immunoprofile of neoglandular epithelium also is consistent with regenerating intestinal epithelium because it showed an increased Ki-67 proliferative index and increased expression of stem cell markers such as Msi-1 and Dcamk11, while still expressing typical intestinal markers such as caudal-related homeobox



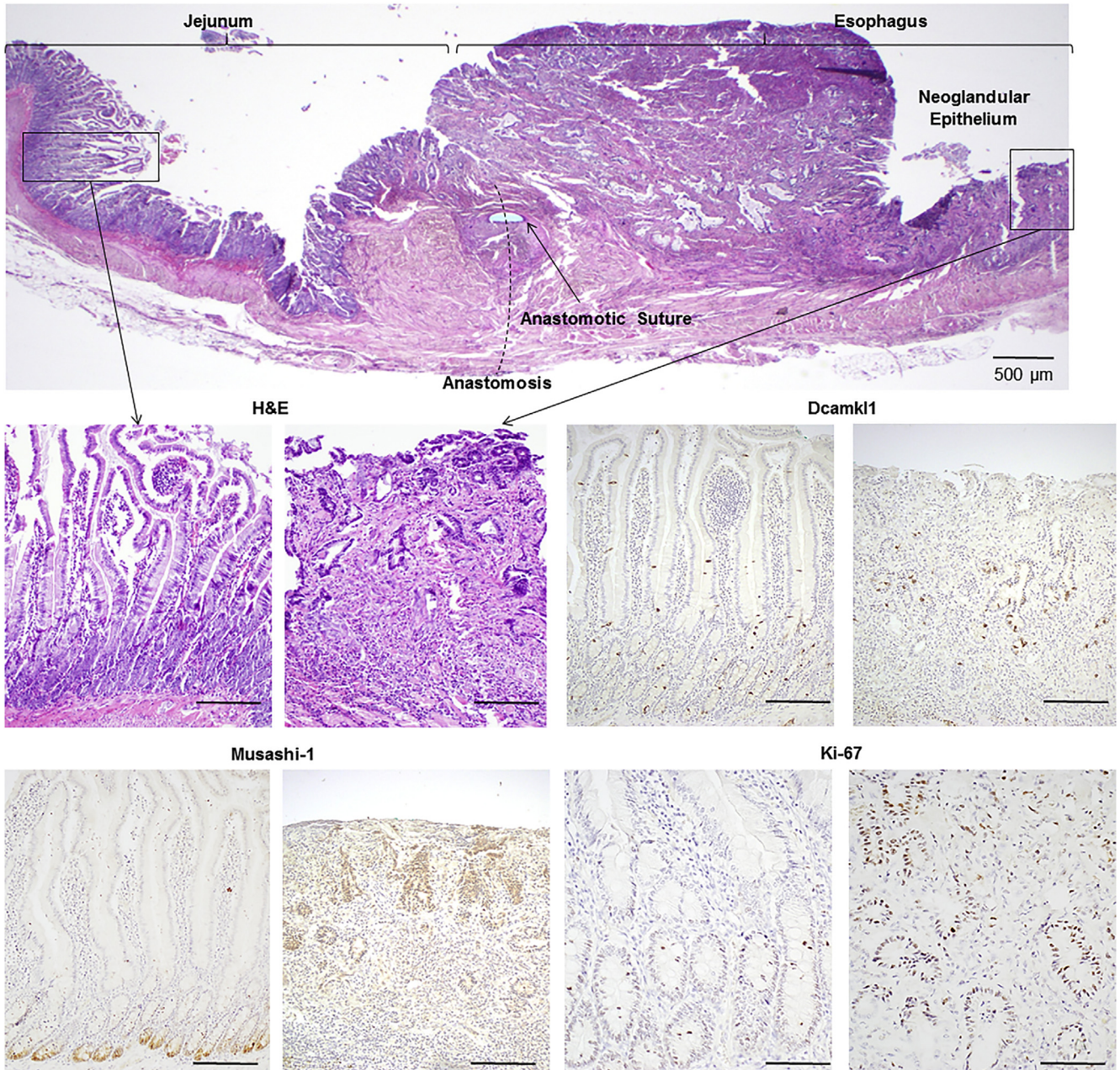


**Figure 5.** The neoglandular epithelium shows a high Ki-67 proliferation rate and expressed markers of intestinal stem cells. Musashi-1 and Dcamk1 immunostaining in native jejunal epithelium (*left side* of each pair) and neoglandular epithelium (*right side* of each pair). The native jejunal epithelium showed nuclear staining for Musashi-1 at the base of the crypts up to approximately the +3 position. Dcamk1 staining was limited predominantly to the crypts. In the neoglandular epithelium, the intensity of Musashi-1 staining was similar to that observed in the deep crypts of the native jejunal epithelium, however, nuclear staining was seen diffusely throughout the neoglandular epithelium. Staining intensity and the location of Dcamk1 in the neoglandular epithelium was similar to that of the native jejunal epithelium. The Ki-67 proliferative index was similar in the basal crypt zone of the native jejunal epithelium and that of the neoglandular epithelium. Scale bar: 100 µm; Ki-67 scale bar: 50 µm.

transcription factor 2, Muc2, and cluster of differentiation 10. Human Barrett’s metaplasia also expresses those intestinal markers, however, unlike human Barrett’s metaplasia, the rat neoglandular epithelium does not express gastric epithelial mucin markers such as Muc5AC and Muc6. Thus, as would be expected for an epithelium arising from

jejunum, rat neoglandular epithelium has intestinal features exclusively, not the combination of intestinal and gastric features found in human Barrett’s esophagus.

Homeostasis of tissues, particularly those located at the junction between different tissue types, is a complex process that is heavily influenced by environmental factors.<sup>24</sup>

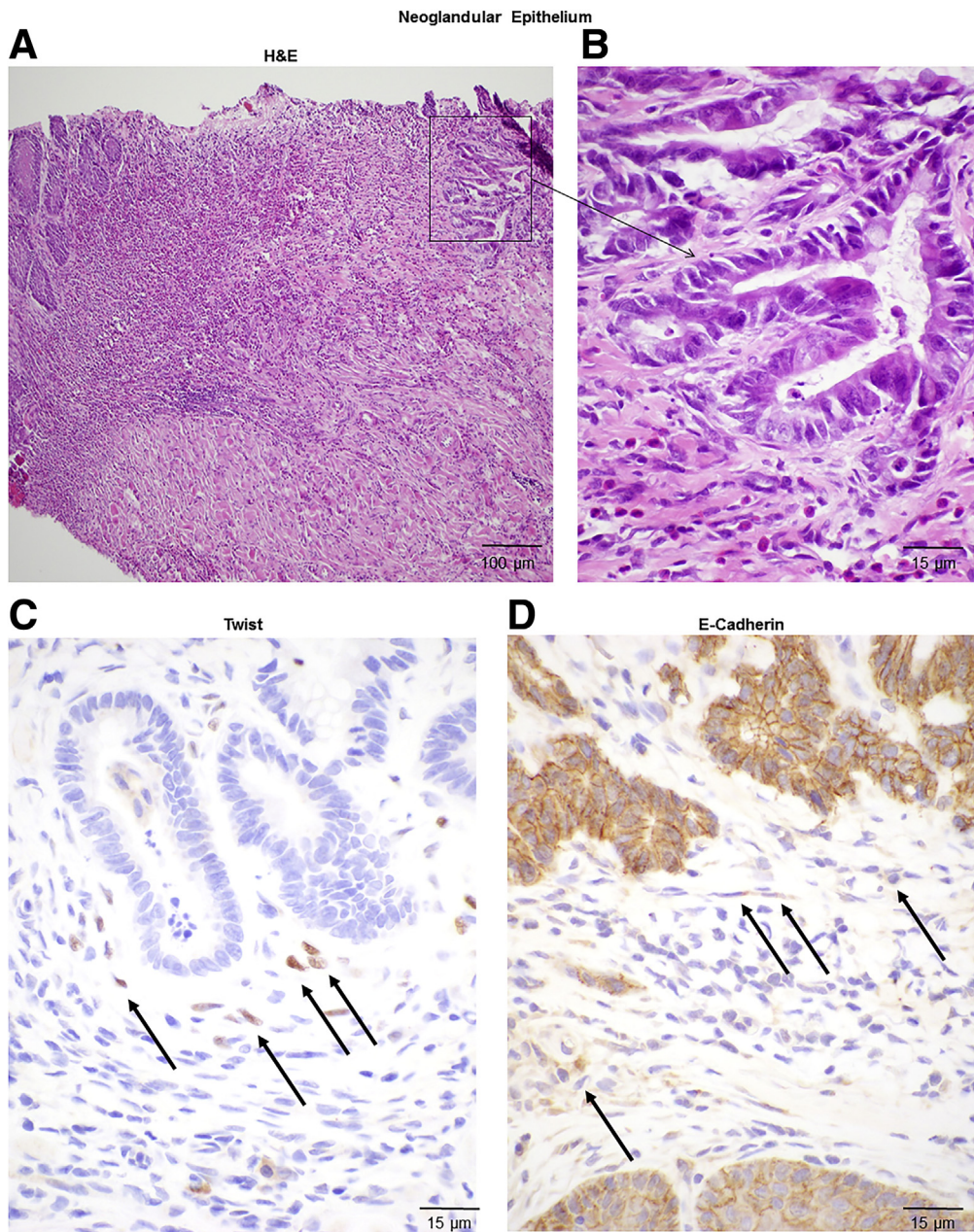


**Figure 6.** Neoglandular epithelium showed markers of EMT by immunostaining. The leading front of neoglandular epithelium showed a population of spindle-shaped mesenchymal-appearing cells at (A) medium power and (B) high power with focal nuclear staining shown at high power for (C) Twist (arrows) and (E) weak but detectable staining for E-cadherin (arrows).

Thus, some cell types can gain a competitive advantage over others as a result of changes in the local environment.<sup>25</sup> Indeed, *in vitro* studies have documented such environmentally influenced competition between Barrett's columnar cells and esophageal squamous cells. When Barrett's cells are co-cultured with esophageal squamous cells, the squamous cells show a competitive advantage in neutral pH culture medium conditions, whereas Barrett's cells out-compete squamous cells in an intermittently acidic environment.<sup>25</sup> In further support of this cell competition concept, Wang et al<sup>7</sup> described a Barrett's-like type of metaplasia developing in mice whose esophageal squamous epithelium is genetically engineered to express diphtheria toxin. They described columnar progenitor cells

located in the gastric cardia that migrate up and proliferate within the toxin-damaged esophagus. We found that the length of neoglandular epithelium (measured from the level of the anastomosis that was identified accurately by the embedded suture) increased linearly over time, progressing up the esophagus at a rate of approximately 0.17 mm/wk. This suggests that, in the setting of chronic GERD induced by esophagojejunostomy, neoglandular cells have a competitive advantage over their squamous counterparts.

As an integral part of wound healing, epithelial cells undergo EMT, in which they show decreased expression of E-cadherin, which is required for normal cell-to-cell adhesion, and morph into mesenchymal-like cells with

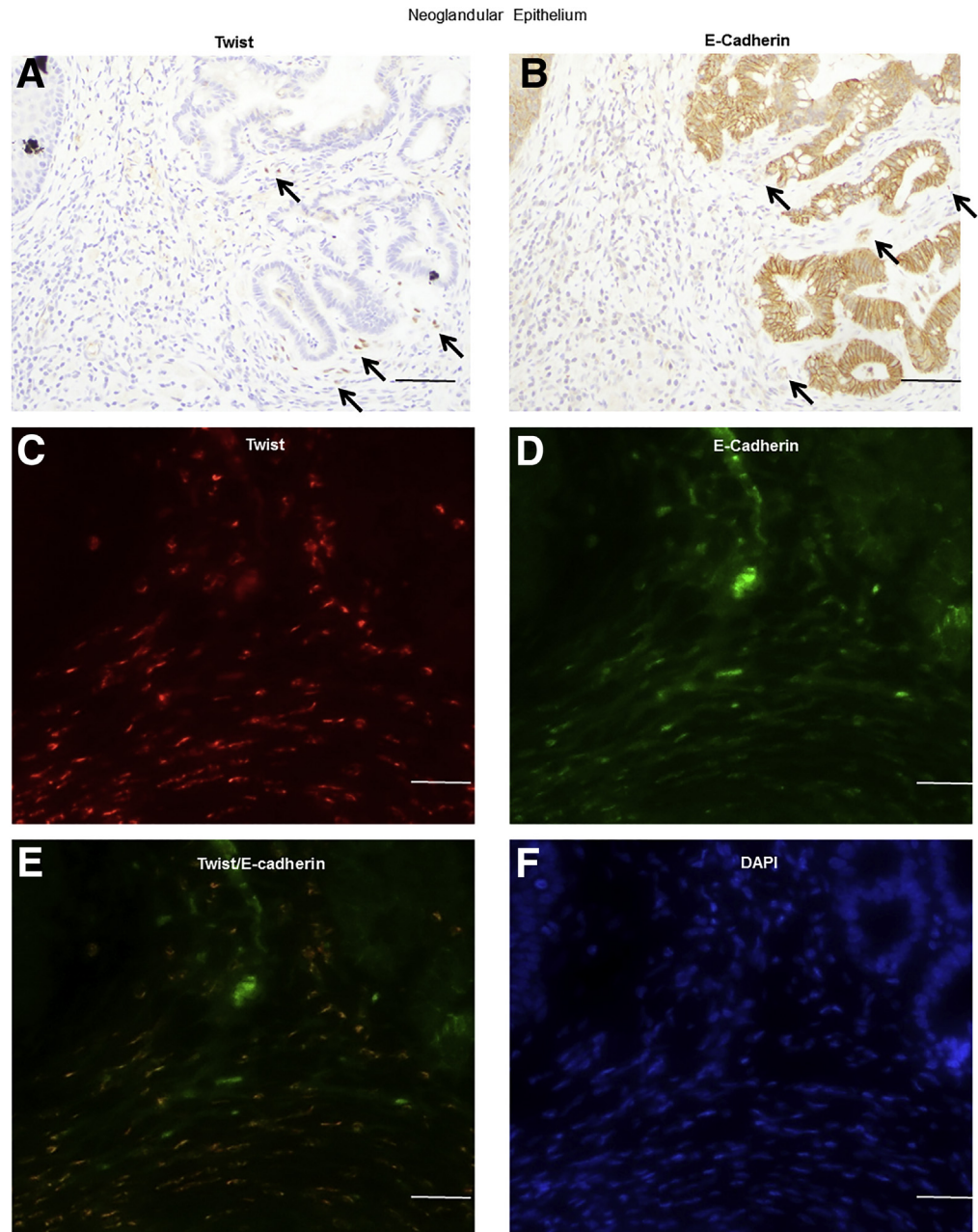


**Figure 7. EMT plays a role in neoglandular re-epithelialization of the esophageal ulcer bed.** The leading front of neoglandular epithelium shows a population of spindle-shaped mesenchymal-appearing cells that contain nuclear staining for (A) Twist (arrows) and (B) weakly positive staining for E-cadherin (arrows) by immunohistochemistry. Scale bars: 50  $\mu\text{mol/L}$ . (C–E) Double immunofluores (C and E) Twist and (D and E) E-cadherin. Scale bar: 25  $\mu\text{mol/L}$ . (F) 4',6-Diamidino-2-phenylindole (DAPI) nuclear staining. Scale bar: 25  $\mu\text{mol/L}$ .

the ability to migrate within mesenchymal tissue.<sup>26</sup> EMT is a reversible process, and the migrated mesenchymal cells can revert back into epithelial cells (mesenchymal-epithelial transition) in distant locations.<sup>26</sup> Our findings of newly formed glands interspersed within the mesenchyme underneath the ulcer bed, and of glands that appeared to grow around squamous islands, suggest that EMT occurs during neoglandular re-epithelialization of the distal esophagus. In support of this concept, the advancing front of the neoglandular epithelium harbors a population of spindle-shaped, mesenchymal-appearing cells that show expression of the EMT transcription factor Twist-1 along with weak expression of the E-cadherin characteristic of epithelial cells. Such a process also might be involved in the development of

subsquamous intestinal-type glands that often are found at the squamocolumnar junction in human beings with Barrett's esophagus. Although EMT also occurs frequently during carcinogenesis, our study cannot assess the potential contribution of reflux-induced EMT to esophageal adenocarcinoma development because our rats did not develop neoplasia during the time frame of the study.

The columnar-lined esophagus that develops in our rat model of reflux esophagitis seems to be an example of a normal (intestinal) epithelium occupying an abnormal location (esophagus), and thus should be considered a metaplasia. However, our finding that this metaplasia develops via wound healing rather than by interconversion between tissue types owing to genetic reprogramming of

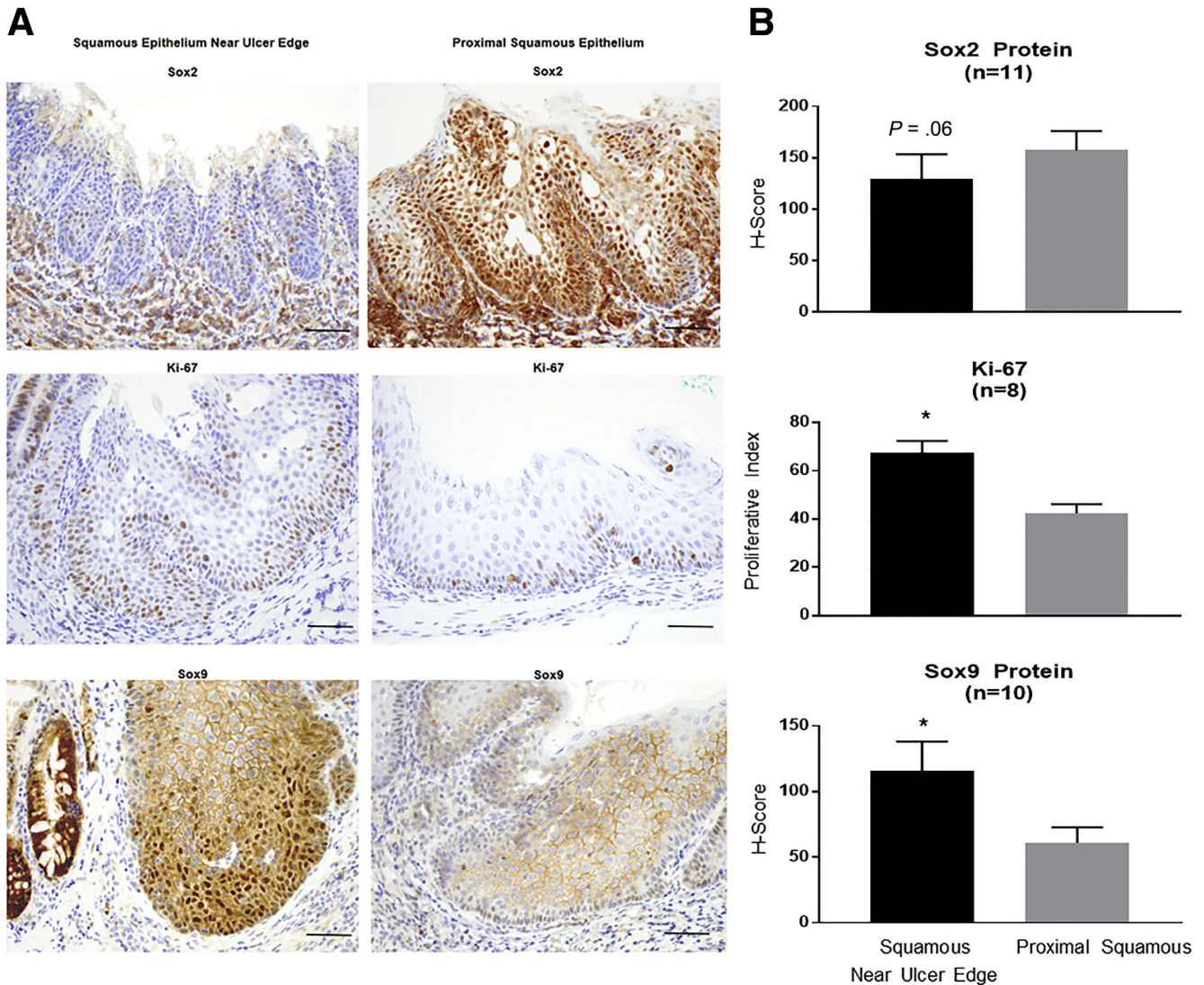


**Figure 8.** Squamous epithelium located within 2 mm of the presumed ulcer edge has a high proliferation rate and expresses high levels of Sox9 compared with squamous epithelium located more than 2 mm from the ulcer edge. (A) Sox2, Ki-67, and Sox9 immunohistochemistry in rat squamous epithelium (left side of each pair) near the ulcer edge and proximal squamous epithelium (right side of each pair) at 10 weeks after surgery. Scale bars: 50  $\mu\text{mol/L}$ . (B) Quantitation of Sox2 and Sox9 staining in rat squamous epithelium using H scores; Ki-67 was quantitated using a proliferative index. Bar graphs show means  $\pm$  SEM. \* $P \leq .05$ .

progenitor cells raises some interesting conceptual issues regarding the definition of the term *metaplasia*. Metaplasia traditionally has been defined as the conversion of one differentiated cell type into another, but Slack<sup>24</sup> argued that it is preferable to use the term *transdifferentiation* for that process and, because metaplastic tissues such as Barrett's esophagus comprise multiple differentiated cell types, to define metaplasia as the conversion of one tissue type into another. However, implicit in Slack's<sup>24</sup> definition is the assumption that metaplasias develop via injury-induced reprogramming of key developmental genes in progenitor cells, resulting in an interconversion of one tissue type into another.<sup>27</sup> Although esophagojejunostomy in rats results in a normal lineage (intestinal epithelium) in an abnormal position (the esophagus), and hence can be

considered a metaplasia, it appears that the neoglandular epithelium developing in this model does so through the upgrowth of immature regenerative intestinal cells via wound repair, rather than through reprogramming of progenitor cells.

In a mouse model of Barrett's esophagus involving esophagogastric jejunostomy, investigators considered their finding of Pdx1 expression in the columnar-lined esophagus as evidence of metaplasia resulting from cellular reprogramming, citing studies suggesting that Pdx1 expression normally is found in the mouse duodenum but not in the jejunum.<sup>15</sup> In our rat model, however, Pdx1 does not appear to be an index of metaplasia caused by cellular programming because we found Pdx1 expression in both jejunal and neoglandular epithelium. It is not clear if this disparity is owing to species differences or

other factors. Nevertheless, our finding of similar Pdx1 expression in neoglandular and native jejunal epithelia supports our contention that metaplasia in this rat model develops by wound healing and not via cellular reprogramming. In contrast, our observation that rat squamous epithelium located at the proximal ulcer edge harbors proliferative cells that expresses Sox9 (a transcription factor expressed in the embryonic, columnar-lined esophagus) but loses expression of Sox2 (a squamous transcription factor of the adult esophagus), suggests the beginning of a metaplastic-like reprogramming on the squamous side of the esophageal ulceration. Nevertheless, these cells retain their squamous phenotype and thus cannot be considered metaplastic or transdifferentiated. Had we extended the duration of our study, it may have been possible to assess whether these squamous cells eventually contribute to a metaplastic, columnar-lined proximal esophagus.

Our findings also raise issues regarding the validity of our rodent model for human Barrett's esophagus. The pathogenesis of human Barrett's esophagus must involve more than simple wound healing from neighboring gastric glands because, in addition to gastric foveolar-type cells, Barrett's epithelium contains intestinal-type cells not normally found in the adjacent stomach. Thus, human Barrett's esophagus appears to be a form of metaplasia that involves reprogramming of key developmental genes in its progenitor cells. However, we speculate that the metaplastic process might well begin with wound healing by adjacent gastric progenitor cells, or by expansion/proliferation of a population of unique embryonic or transitional basal cells recently described in the columnar epithelium located at the squamocolumnar junction in mice and human beings. These progenitor cells may expand and proliferate to heal the wound by initially covering it with genetically unaltered columnar cells. Later, in the setting of ongoing GERD, these cells might undergo genetic reprogramming to produce a columnar epithelium with intestinal features.<sup>28,29</sup> In rodent models, furthermore, it is not possible to assess any contribution of submucosal glands to the development of columnar-lined esophagus because the rodent esophagus lacks submucosal glands. Despite these limitations, we believe that our model provides evidence to suggest that the pathogenesis of human Barrett's esophagus begins as a wound healing process, especially at the distal edge of the ulcers that abut columnar epithelium.

In conclusion, using a rat model of reflux esophagitis via surgical esophagojejunostomy, we have shown that a metaplastic, columnar-lined esophagus develops via a wound healing process, and not via genetic reprogramming of progenitor cells. Re-epithelialization of ulcerated squamous mucosa at the level of the anastomosis occurs via proliferation and expansion of immature glands that arise directly from adjacent jejunal crypts, and the neoglandular epithelium shows an immunoprofile similar to that of the native proliferating crypt base jejunal epithelium. Moreover, the growth of immature-appearing glands that express both Twist-1 and E-cadherin into the deep mesenchyme of the ulcerated distal esophagus, and the apparent extension of neoglandular epithelium around squamous islands, all suggest an important role for EMT in this esophageal wound healing process. The length of neoglandular

epithelium increased linearly over time, consistent with a competition event in which neoglandular cells have an advantage over their squamous counterparts in the setting of GERD induced by esophagojejunostomy. Further studies are needed in patients with GERD to determine whether the pathogenesis of Barrett's esophagus in human beings begins as a wound healing process.

## Materials and Methods

### Animals

We used 78 Sprague-Dawley rats (age, 6 wk; average body weight, 250 ± 22 g; Charles River Laboratory, Wilmington, MA) for these studies. The animals were kept in conventional housing (12-hour light/dark cycle; ambient temperature, 72°F), and were fed standard rat chow with water given ad libitum; rat chow was withheld 1 day before surgery. Rats were anesthetized with intraperitoneal injections of ketamine (75 mg/kg) and xylazine (12 mg/kg). After surgery, rats were weighed and their condition was assessed daily for 5 days, then once every 2 weeks. Animals were euthanized by carbon dioxide asphyxiation with bilateral thoracotomies if they became ill or lost more than 20% of their preoperative body weight. The study protocol was approved by the Dallas Veteran Affairs Medical Center Institutional Animal Care and Use Committee.

### Rat Model of Reflux Esophagitis (Esophagojejunostomy)

Gastroesophageal reflux was induced by fashioning an esophagojejunostomy as previously described by Levrat et al<sup>10</sup> in 60 animals. In brief, using a small upper midline laparotomy, the stomach was mobilized and the gastroesophageal junction was ligated with 5-0 polypropylene suture. The esophagus was divided just proximal to the suture, an end-to-side esophagojejunal anastomosis was performed using 7-0 polypropylene suture, and the laparotomy incision was closed using 5-0 polypropylene suture. For controls, we performed a sham surgery comprising anesthesia, celiotomy, and dissection of the gastroesophageal junction without esophageal transection or esophagojejunostomy. Animals were fed a liquid diet of Ensure (Abbott Nutrition, Columbus, OH) for 5 days after surgery, and then restarted on standard rat chow. The preoperative and postoperative care of the esophagojejunostomy and sham-operated control rats was identical.

The overall mortality rate for the esophagojejunal anastomosis group was 13%. Deaths resulted from aspiration (5 animals), bowel obstruction from ingestion of a foreign body (2 animals), and evisceration in the immediate postoperative period (1 animal), leaving 52 animals with an esophagojejunal anastomosis available for study. There were no deaths in the sham-operated group, leaving 18 control animals available for study.

### Tissue Handling and Pathologic Evaluation

Groups of at least 5 animals (total, 60 rats) that had esophagojejunostomy were euthanized at postoperative

**Table 1.** Antibodies Used

Antibody	Source information: catalog number; company	Dilution	Antigen retrieval solution
CDX2	A300-691A; Bethyl Labs (Montgomery, TX)	1:100	H2
MUC2	NCL-MUC-2; Leica Biosystems, Inc	1:50	H2
Villin	IM0258; Immunotech (Indianapolis, IN)	1:50	H1
CD10	VP-C328; Vector Labs (Burlingame, CA)	1:20	H1
MUC5AC	18-2261; Invitrogen (Waltham, MA)	1:100	H1
MUC6	ab49462; Abcam (Cambridge, MA)	1:100	H2
p63	CM163A; Biocare Medical (Pacheco, CA)	1:25	H2
Das-1	Laboratory of Kiron M. Das, Rutgers-Robert Wood Johnson University	1:1000	H2
Musashi-1	ab52865; Abcam	1:150	H1
DCAMKL1	ab31704; Abcam	1:100	H1
Twist-1	ab50887; Abcam	1:50, IHC 1:50, IF	H1
Snail	Ab53519; Abcam	1:2000	H2
E-cadherin	610181; BD Biosciences (San Jose, CA)	1:100, IHC 1:100, IF	H1
N-cadherin	ab18203; Abcam	1:250	H1
SOX2	ab97959; Abcam	1:100	H1
SOX9	5535; EMD Millipore (Billerica, MA)	1:100	H2
PDX1	ab47267; Abcam	1:500	H1
Ki-67	SKU 325; Biocare Medical	1:200	H2

CD, cluster of differentiation; IF, immunofluorescence; IHC, immunohistochemistry.

weeks 2, 4, 6, 8, 10, 12, 16, 24, and 32; 2 sham-operated control rats were euthanized at each corresponding time point. The esophagus, including the esophagojejunal anastomosis, was removed en bloc and opened longitudinally. Sample strips of esophagus and jejunum were snap frozen and stored in liquid nitrogen. The remaining esophagus was pinned flat on a corkboard and fixed in 10% buffered formalin for 24 hours. The esophagus was cut into 2-mm-wide sections, which were oriented and placed into cassettes before paraffin fixation. Serial sections (4- $\mu$ m-thick) were mounted on glass slides and stained with H&E for histologic evaluation. Two gastrointestinal pathologists (R.D.O. and A.T.A.), who were blinded to surgical group, evaluated the esophageal specimens for a variety of histologic features in the squamous epithelium, ulcer base, and columnar epithelium at the esophagojejunal anastomosis. The squamous epithelium was evaluated for the presence and degree of esophagitis, surface erosion or ulceration, and type and degree of inflammatory infiltrate. Specific histologic features such as the degree of basal cell hyperplasia, papillary hyperplasia, and intercellular edema (spongiosis) also were graded on a semiquantitative scale (scale, 0–3). The portion of mucosa that was ulcerated was evaluated for the presence of residual islands of squamous mucosa surrounded by ulcer, and, in particular, for the type and characteristics of the epithelium at the proximal and distal edges of the ulcer where mucosal healing was assumed to occur. At the distal ulcer/jejunal mucosa interface, the jejunal epithelium was evaluated for characteristics of the villi and crypts, and for the type, pattern, and degree

of regenerating columnar epithelium at the level of the esophagojejunal anastomosis. The location of the esophagojejunal anastomosis was identified histologically by noting the specific location of the embedded sutures used for the anastomosis and by noting the location of change in the characteristics and thickness of the muscularis propria.

### Quantification of Esophageal Re-epithelization

To quantify the length of the neoglandular epithelium in the distal esophagus, we measured the distance from the proximal leading edge of the neoglandular epithelium to the anastomosis (the latter indicated by the location of the anastomotic suture) in 37 animals at times ranging from 2 to 32 weeks after surgery. For the remaining 15 animals, either fragmentation or suboptimal orientation of the histologic sections precluded determination of this measurement.

### Immunohistochemistry and Immunofluorescence

Tissue sections were stained on a Leica Bond III autostainer (Leica Biosystems, Inc, Buffalo Grove, IL), using their Polymer Refine Detection Kit (cat DS9800). Heat retrieval was performed using either the Bond Epitope Retrieval Solution 1 (H1), pH 6.0 (cat AR9961), or the Bond Epitope Retrieval Solution 2 (H2), pH 9.0 (cat AR9640). Slides were incubated in the primary antibody for 30 minutes (Table 1 lists the dilutions, suppliers, and antigen retrieval formula used), followed by the secondary polymer for 15 minutes; 3,3'-diaminobenzidine tetrahydrochloride was used for visualization. Appropriate positive and negative controls

were used. Staining intensity was quantitated using an H-score technique.<sup>30,31</sup> In brief, staining intensity was scored on a scale of 0–3 (0, no staining; 1, faint staining; 2, moderate staining; and 3, strong staining), and the percentage of cells at each staining intensity was determined. The H-score was calculated using the following formula:  $3 \times (\% \text{ cells with strong staining}) + 2 \times (\% \text{ cells with moderate staining}) + 1 \times (\% \text{ cells with weak staining})$ ; and the possible score range was 0–300. Tissues were evaluated and scored by 2 expert gastrointestinal pathologists (A.T.A. and R.D.O.), who were blinded to the experimental groups. Tissue sections containing both neoglandular epithelium and jejunum were stained for pancreatic and duodenal homeobox 1 (Pdx1). Immunofluorescence double staining for Twist-1 and E-cadherin was performed on the Leica Bond III automated staining platform. Heat-induced antigen retrieval was performed using citrate for 30 minutes. Antibodies were incubated for 30 minutes each in series, first Twist-1 at a 1:50 dilution, followed by Leica post primary and polymer followed by Thermo Scientific (Waltham, MA) 488 tyramide (B40953), then E-cadherin at a 1:100 dilution followed by Leica post primary and polymer followed by Thermo Scientific 594 tyramide (B40957). Slides were counterstained with 4',6-diamidino-2-phenylindole (R37606; Life Technologies, Carlsbad, CA) for 10 minutes.

### Statistical Analyses

Quantitative H score data are expressed as means  $\pm$  SEM. Statistical analyses were performed using a paired Student *t* test using the InStat for Windows statistical software package (GraphPad Software, San Diego, CA). Correlations between data were analyzed using the Pearson linear correlation model using the Prism 7.00 statistical software package (GraphPad Software). *P* values  $\leq .05$  were considered significant for all analyses. All authors had access to the study data and reviewed and approved the final manuscript.

### References

- Hayeck TJ, Kong CY, Spechler SJ, Gazelle GS, Hur C. The prevalence of Barrett's esophagus in the US: estimates from a simulation model confirmed by SEER data. *Dis Esophagus* 2010;23:451–457.
- Rex DK, Cummings OW, Shaw M, Cumings MD, Wong RK, Vasudeva RS, Dunne D, Rahmani EY, Helper DJ. Screening for Barrett's esophagus in colonoscopy patients with and without heartburn. *Gastroenterology* 2003;125:1670–1677.
- Thrift AP, Pandeya N, Whiteman DC. Current status and future perspectives on the etiology of esophageal adenocarcinoma. *Front Oncol* 2012;2:11.
- Spechler SJ, Souza RF. Barrett's esophagus. *N Engl J Med* 2014;371:836–845.
- Wang DH, Souza RF. Transcommitment: paving the way to Barrett's metaplasia. *Adv Exp Med Biol* 2016;908:183–212.
- Quante M, Bhagat G, Abrams JA, Marache F, Good P, Lee MD, Lee Y, Friedman R, Asfaha S, Dubeykovskaya Z, Mahmood U, Figueiredo JL, Kitajewski J, Shawber C, Lightdale CJ, Rustgi AK, Wang TC. Bile acid and inflammation activate gastric cardia stem cells in a mouse model of Barrett-like metaplasia. *Cancer Cell* 2012;21:36–51.
- Wang X, Ouyang H, Yamamoto Y, Kumar PA, Wei TS, Dagher R, Vincent M, Lu X, Bellizzi AM, Ho KY, Crum CP, Xian W, McKeon F. Residual embryonic cells as precursors of a Barrett's-like metaplasia. *Cell* 2011;145:1023–1035.
- Jiang M, Li H, Zhang Y, Yang Y, Lu R, Liu K, Lin S, Lan X, Wang H, Wu H, Zhu J, Zhou Z, Xu J, Lee DK, Zhang L, Lee YC, Yuan J, Abrams JA, Wang TC, Sepulveda AR, Wu Q, Chen H, Sun X, She J, Chen X, Que J. Transitional basal cells at the squamous-columnar junction generate Barrett's oesophagus. *Nature* 2017;550:529–533.
- Sarosi G, Brown G, Jaiswal K, Feagins LA, Lee E, Crook TW, Souza RF, Zou YS, Shay JW, Spechler SJ. Bone marrow progenitor cells contribute to esophageal regeneration and metaplasia in a rat model of Barrett's esophagus. *Dis Esophagus* 2008;21:43–50.
- Levrat M, Lambert R, Kirshbaum G. Esophagitis produced by reflux of duodenal contents in rats. *Am J Dig Dis* 1962;7:564–573.
- Goldstein SR, Yang GY, Curtis SK, Reuhl KR, Liu BC, Mirvish SS, Newmark HL, Yang CS. Development of esophageal metaplasia and adenocarcinoma in a rat surgical model without the use of a carcinogen. *Carcinogenesis* 1997;18:2265–2270.
- Buttar NS, Wang KK, Leontovich O, Westcott JY, Pacifico RJ, Anderson MA, Krishnadath KK, Lutzke LS, Burgart LJ. Chemoprevention of esophageal adenocarcinoma by COX-2 inhibitors in an animal model of Barrett's esophagus. *Gastroenterology* 2002;122:1101–1112.
- Fein M, Peters JH, Chandrasoma P, Ireland AP, Oberg S, Ritter MP, Bremner CG, Hagen JA, DeMeester TR. Duodenoesophageal reflux induces esophageal adenocarcinoma without exogenous carcinogen. *J Gastrointest Surg* 1998;2:260–268.
- Badve S, Logdberg L, Sokhi R, Sigal SH, Botros N, Chae S, Das KM, Gupta S. An antigen reacting with das-1 monoclonal antibody is ontogenically regulated in diverse organs including liver and indicates sharing of developmental mechanisms among cell lineages. *Pathobiology* 2000;68:76–86.
- Terabe F, Aikou S, Aida J, Yamamichi N, Kaminishi M, Takubo K, Seto Y, Nomura S. Columnar metaplasia in three types of surgical mouse models of esophageal reflux. *Cell Mol Gastroenterol Hepatol* 2017;4:115–123.
- Seno H, Miyoshi H, Brown SL, Geske MJ, Colonna M, Stappenbeck TS. Efficient colonic mucosal wound repair requires Trem2 signaling. *Proc Natl Acad Sci U S A* 2009;106:256–261.
- Vega KJ, May R, Sureban SM, Lightfoot SA, Qu D, Reed A, Weygant N, Ramanujam R, Souza R, Madhoun M, Whorton J, Anant S, Meltzer SJ, Houchen CW. Identification of the putative intestinal stem cell marker doublecortin and CaM kinase-like-1 in Barrett's esophagus and esophageal adenocarcinoma. *J Gastroenterol Hepatol* 2012;27:773–780.

18. Mari L, Milano F, Parikh K, Straub D, Everts V, Hoeben KK, Fockens P, Buttar NS, Krishnadath KK. A pSMAD/CDX2 complex is essential for the intestinalization of epithelial metaplasia. *Cell Rep* 2014;7:1197–1210.
19. Wang DH, Clemons NJ, Miyashita T, Dupuy AJ, Zhang W, Szczepny A, Corcoran-Schwartz IM, Wilburn DL, Montgomery EA, Wang JS, Jenkins NA, Copeland NA, Harmon JW, Phillips WA, Watkins DN. Aberrant epithelial-mesenchymal Hedgehog signaling characterizes Barrett's metaplasia. *Gastroenterology* 2010;138:1810–1822.
20. Tarnawski AS, Ahluwalia A. Molecular mechanisms of epithelial regeneration and neovascularization during healing of gastric and esophageal ulcers. *Curr Med Chem* 2012;19:16–27.
21. Chen X, Yang G, Ding WY, Bondoc F, Curtis SK, Yang CS. An esophagogastrroduodenal anastomosis model for esophageal adenocarcinogenesis in rats and enhancement by iron overload. *Carcinogenesis* 1999;20:1801–1808.
22. Su Y, Chen X, Klein M, Fang M, Wang S, Yang CS, Goyal RK. Phenotype of columnar-lined esophagus in rats with esophagogastrroduodenal anastomosis: similarity to human Barrett's esophagus. *Lab Invest* 2004;84:753–765.
23. Martin P. Wound healing—aiming for perfect skin regeneration. *Science* 1997;276:75–81.
24. Slack JM. Metaplasia and transdifferentiation: from pure biology to the clinic. *Nat Rev Mol Cell Biol* 2007;8:369–378.
25. Merlo LM, Kosoff RE, Gardiner KL, Maley CC. An in vitro co-culture model of esophageal cells identifies ascorbic acid as a modulator of cell competition. *BMC Cancer* 2011;11:461.
26. Kalluri R, Weinberg RA. The basics of epithelial-mesenchymal transition. *J Clin Invest* 2009;119:1420–1428.
27. Shen CN, Burke ZD, Tosh D. Transdifferentiation, metaplasia and tissue regeneration. *Organogenesis* 2004;1:36–44.
28. Dias Pereira A, Chaves P. Columnar-lined oesophagus without intestinal metaplasia: results from a cohort with a mean follow-up of 7 years. *Aliment Pharmacol Ther* 2012;36:282–289.
29. O'Riordan JM, Tucker ON, Byrne PJ, McDonald GS, Ravi N, Keeling PW, Reynolds JV. Factors influencing the development of Barrett's epithelium in the esophageal remnant postesophagectomy. *Am J Gastroenterol* 2004;99:205–211.
30. Hirsch FR, Varella-Garcia M, Bunn PA Jr, Di Maria MV, Veve R, Bremmes RM, Baron AE, Zeng C, Franklin WA. Epidermal growth factor receptor in non-small-cell lung carcinomas: correlation between gene copy number and protein expression and impact on prognosis. *J Clin Oncol* 2003;21:3798–3807.
31. John T, Liu G, Tsao MS. Overview of molecular testing in non-small-cell lung cancer: mutational analysis, gene copy number, protein expression and other biomarkers of EGFR for the prediction of response to tyrosine kinase inhibitors. *Oncogene* 2009;28(Suppl 1):S14–S23.

---

Received December 4, 2017. Accepted June 19, 2018.

#### Correspondence

Address correspondence to: Rhonda F. Souza, MD, Center for Esophageal Research, Baylor University Medical Center, 2 Hoblitzelle, Suite 250, 3500 Gaston Avenue, Dallas, Texas 75246. e-mail: [Rhonda.Souza@BSWHealth.org](mailto:Rhonda.Souza@BSWHealth.org).

#### Acknowledgments

The authors thank Elizabeth Cook, HT (ASCP), Histopathology Technician at the Center for Esophageal Research, Baylor University Medical Center and Baylor Scott and White Research Institute for assistance in the preparation of tissue samples; the Dana-Farber/Harvard Cancer Center in Boston, MA for the use of the Specialized Histopathology Core; and core technologists Ashley Pelton and Benjamin Ferland, who provided the immunohistochemical and immunofluorescence staining service. The Dana-Farber/Harvard Cancer Center is supported in part by a National Cancer Institute Cancer Center Support Grant National Institutes of Health 5 P30 CA06516.

#### Author contributions

Agoston T. Agoston was responsible for the study design, technical and material support, analysis and interpretation of data, critical revision of the manuscript, important intellectual content, and drafting the manuscript; Thai H. Pham was responsible for the study design, technical and material support, analysis and interpretation of data, critical revision of the manuscript, important intellectual content, and drafting the manuscript; David H. Wang was responsible for technical and material support and important intellectual content; Kiron M. Das was responsible for technical and material support and important intellectual content; Robert D. Odze was responsible for the analysis and interpretation of data, critical revision of the manuscript, and important intellectual content; Stuart J. Spechler was responsible for the study concept, analysis, and interpretation of data, critical revision of the manuscript, and important intellectual content; and Rhonda F. Souza was responsible for the study concept/design, analysis and interpretation of data, critical revision of the manuscript, important intellectual content, and drafting the manuscript.

#### Conflicts of interest

The authors disclose no conflicts.

#### Funding

This work was supported by National Institutes of Health grants R01-DK63621, R01-DK103598, and R21DK111369 (R.F.S. and S.J.S.), and R01-DK097340 (D.H.W.), and by the Baylor Scott and White Research Institute. The contents do not represent the views of the US Department of Veterans Affairs or the United States Government.